Route toward semiconductor magnonics: Light-induced spin-wave nonreciprocity in a YIG/GaAs structure

A. V. Sadovnikov,[1,2,*] E. N. Beginin,[1] S. E. Sheshukova,[1] Yu. P. Sharaevskii,[1] A. I. Stognij,[3] N. N. Novitski,[3] V. K. Sakharov,[4] Yu. V. Khivintsev,[4] and S. A. Nikitov[1,2]

[1]*Laboratory "Metamaterials," Saratov State University, Saratov 410012, Russia*
[2]*Kotel'nikov Institute of Radioengineering and Electronics, RAS, Moscow 125009, Russia*
[3]*Scientific-Practical Materials Research Center, National Academy of Sciences of Belarus, 220072 Minsk, Belarus*
[4]*Kotel'nikov SBIRE RAS and Saratov State University, Saratov 410019, Russia*

We demonstrate laser-induced nonreciprocity of spin waves in the ferromagnetic-semiconductor structure. Surface spin waves in yttrium iron garnet film grown at the top of *n*-type gallium arsenide substrate were studied by means of Brillouin light-scattering spectroscopy. It is shown that spin-wave dispersion can be modified in a controlled manner by laser radiation. We observe the difference of up to 225 MHz when comparing the frequencies of counterpropagating spin waves. We attribute this frequency shift to the mutual influence of nonreciprocal spin-wave modal profiles and differences in magnetic anisotropies at two film surfaces as the result of laser-induced conductivity variation in GaAs substrate. We propose a simple model based on analytical dipole theory to describe the induced spin-wave nonreciprocity. Our results show the possibility of integration of magnonics and semiconductor electronics on the base of YIG/GaAs structures.

I. INTRODUCTION

The most important parameters of the conventional complementary metal-oxide-semiconductor (CMOS)-based electronics [1] such as high processing speed, small element size, low power consumption, and low heat radiation, have fundamental physical limitations. As the size of devices becomes smaller, tunneling and leakage currents grow, and dielectric and wiring materials cannot provide reliable insulation and conduction. An increased number of transistors integrated per unit-area demands larger power consumption and higher thermal dissipation. One of the alternative concepts having the ability to overcome the above-mentioned issues is insulator-based magnonics [2–7], whose main principle lies in using spin waves (SW) or magnons [8] instead of electrons as information carriers [9,10]. Magnonic networks form all-magnonic devices that can act as separate units in functional microwave devices [6,11–16].

An important step towards the integration of magnonic networks and CMOS-based electronics is the fabrication of the magnonic complement to semiconductor devices. Yttrium iron garnet ($Y_3Fe_5O_{12}$, YIG), with extremely low losses for propagating spin waves, is the most appropriate material for the emerging technologies of spintronics and magnonics due to excitation of magnetization dynamics by pure spin currents and spin-transfer torque, as it was shown recently [17–21]. However, integration of magnonic functional structures into semiconductor-based electronics faces some problems, the main one being the incompatibility of substrates typically used in YIG magnonics and conventional CMOS-

based electronics. YIG films for magnonic devices are usually grown on gadolinium gallium garnet (GGG) substrates by liquid phase epitaxy, radio frequency magnetron sputtering [22,23], ion-beam evaporation [24,25], or pulsed laser deposition [26,27], whereas in the CMOS-based electronics, gallium arsenide (GaAs) is one of the most utilized types of substrates, as it has a high mobility of charge carriers and a direct and wide band gap. Therefore, YIG structures on GaAs substrates are promising candidates for the purpose of magnonic and spintronic element integration into the semiconductor architecture. The possibility of such integration follows from the permanent progress that is shown by efforts in the technology development of YIG-semiconductor systems, for example, ones on the base of GaN [28,29] and Si [25] substrates.

Moreover, the combination of magnetic layers with semiconductor quantum dots is the best choice for possible high-speed photon generation induced by magnetic field and having emission rates up to several hundreds of GHz [30,31].

The nonreciprocal propagation [32–39] of spin waves in thin films occurs in the Damon-Eschbach (DE) [40] configuration when both the spin-wave vector *k* and the direction of magnetization *M* lie in the film plane perpendicular to each other. In this configuration, the modal profiles of counterpropagating magnetostatic surface waves (MSSW) can differ considerably due to different magnetic surface anisotropies at two film surfaces [41–43] or the influence of metallic planes in the vicinity of the film surface [44–46]. The frequencies of two counterpropagating spin waves also differ from each other as soon as the top/bottom symmetry of the ferromagnetic film is broken due to interfacial Dzyaloshinskii-Moria interaction [47], for example, or in the case of a double-layer magnetic film [43].

*sadovnikovav@gmail.com

One of the alternative methods of control over nonreciprocal features of spin waves can consist in the combination of a double-layer magnetic structure with semiconductor substrate and light-induced variation of the GaAs semiconductor substrate properties [48,49].

In this article we present our results of experimental study of spin-wave excitations in YIG film on GaAs substrate performed with Brillouin light-scattering (BLS) spectroscopy and ferromagnetic resonance (FMR) techniques. We show that the spin-wave dispersion can be modified in a controlled manner by illumination of the semiconductor substrate with the infrared laser radiation. Thus, the advantage of ferromagnetic/semiconductor structures as compared to conventional YIG based units is the light control over the spin-wave dispersion and nonreciprocity. This may be the first experimental step in integrated semiconductor magnonics on the base of YIG/GaAs structures.

II. SAMPLE PREPARATION AND FMR MEASUREMENT

YIG film was deposited on 400-μm-thick lightly doped n-type GaAs(100) substrates by the double-ion-beam sputter-deposition method in Ar+O_2 atmosphere [25]. The $Y_3Fe_5O_{12}$ ceramic disk with diameter of 100 mm was used as the target. In order to reduce elastic deformation and diffusion of Ga and As ions into the YIG layer, we sputtered the amorphous AlO_x layer with a thickness of 4 nm on GaAs [Fig. 1(a)]. Then the thin buffer YIG layer was sputtered.

TABLE I. Results of FMR experiment.

Parameters	$H_\parallel$	$H_\perp$
Resonance	$H_{\parallel 1} = 2.895$	$H_{\perp 1} = 4.882$
magnetic field (kOe)	$H_{\parallel 2} = 3.001$	$H_{\perp 2} = 4.707$
Full width at	$\Delta H_{\parallel 1} = 223$	$\Delta H_{\perp 1} = 52$
half maximum (Oe)	$\Delta H_{\parallel 2} = 134$	$\Delta H_{\perp 2} = 198$
Effective	$4\pi M_{\parallel 1} = 1.397$	$4\pi M_{\perp 1} = 1.357$
magnetization (kG)	$4\pi M_{\parallel 2} = 1.139$	$4\pi M_{\perp 2} = 1.182$

After annealing in the quasi-impulse regime during 2 min at 590 °C in N_2 atmosphere with a pressure of 0.1 Torr, the buffer YIG layer obtained the polycrystalline structure. This layer was then planarized by the low-energy (400-eV) oxygen-ion-beam sputtering in order to decrease the stress tension and amount of dislocations. Such planarization made the sample's surface suitable for deposition of the main YIG layer without lattice and thermal mismatch and interdiffusion on the interface. We next obtained images of the YIG film surface and the cross section of the whole YIG/GaAs structure by means of focused-ion-beam milling in Helios NanoLab 600 [see the insets to Fig. 1(a)]. These pictures reveal the polycrystalline structure of YIG with crystallite size from 20 to 60 nm. We could define the thicknesses of both YIG films as $d_1 = 50 \pm 5$ nm and $d_2 = 60 \pm 5$ nm. It should be also noted that using the x-ray 2θ-ω (out-of-plane) diffraction we revealed the $Y_3Fe_5O_{12}$ peak besides the GaAs substrate reflection. Analysis of the x-ray diffraction pattern indicated a homogeneous phase of YIG structure similar to the bulk media signal.

The FMR spectrum was measured by the conventional cavity FMR method at fixed frequency $f_r = 9.87$ GHz and at room temperature for two orientations of applied magnetic field (in-plane and out-of-plane) ranging from 0.1 to 5.5 kOe. The first derivative of the FMR curve is depicted in the inset of Figs. 1(b) and 1(c). To reveal the FMR peaks position H_r of each sublayer we performed the Lorentzian decomposition of the FMR curve. We used two Lorentzian functions (dashed blue and dotted red curves) in order to properly fit the FMR spectrum (black solid line) and define the resonance field and linewidth for each magnetic layer. It is worth noting that the linewidth of the FMR curve was formed both by relaxation of spin excitations and by magnetic inhomogeneity of our magnetic film. The results of FMR measurement are summarized in Table I. The effective magnetization of each layer can be estimated as

$$4\pi M_\perp = H_r - f_r/\gamma, \quad 4\pi M_\parallel = \frac{(f_r/\gamma)^2 - H_r^2}{H_r}, \quad (1)$$

where $\gamma/(2\pi) = 2.83$ GHz/kOe is the gyromagnetic ratio for YIG. Thus we obtained the following parameters of each YIG layer: $4\pi M_{\mathrm{eff}1} = 4\pi M_1 = 1.139$ kG and $4\pi M_{\mathrm{eff}2} = 4\pi M_2 = 1.397$ kG.

III. BRILLOUIN LIGHT SCATTERING MEASUREMENT AND LASER INDUCED SPIN-WAVE NONRECIPROCITY

Next, we used the BLS technique [50,51] to investigate the spin-wave spectrum in the YIG/GaAs structure. BLS
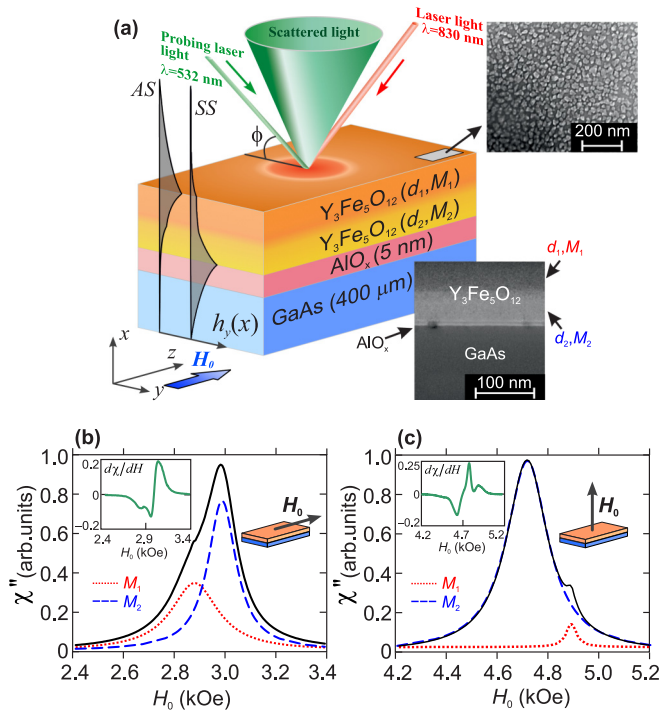
FIG. 1. (a) Schematic view of YIG/GaAs structure and cartoon of BLS experiment. BLS measurement was performed in the backscattering configuration. Insets: Cross section (bottom) and surface (top) of YIG/GaAs. (b) FMR spectrum of YIG/GaAs structure at in-plane and (c) perpendicular-to-plane magnetic field orientation taken at frequency $f = 9.87$ GHz. Inset: FMR derivative absorption spectra.
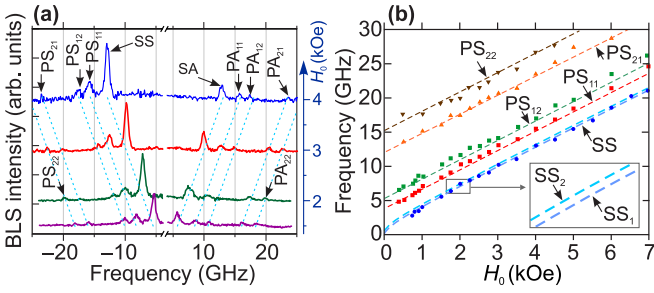
FIG. 2. (a) BLS spectra of spin waves in YIG/GaAs structure acquired with variation of applied external field. (b) Measured spin-wave frequencies as a function of the magnetic field. The dashed lines represent frequencies calculated with Eq. (2). Splitting of the SS mode is shown in the inset.
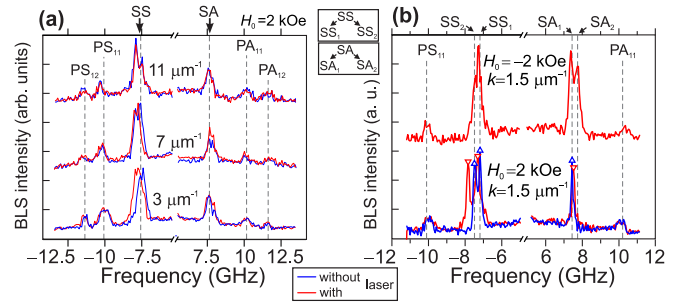

FIG. 3. (a) BLS spectra of YIG/GaAs structure for different transferred wave vectors in the external field of 2 kOe. The vertical dashed lines indicate the position of DE modes and PSSW modes at wave number 3 μm^{-1}. (b) BLS spectra acquired at negative and positive values of magnetic field and at $k = 1.5$ μm^{-1}. Blue and red curves in (a) and (b) correspond to the spectra without and with IR laser radiation, respectively.

combines the possibility to study the spin-wave modes, which are excited thermally, and dynamics of magnetic systems in the frequency range up to several GHz. Thus, due to the very high sensitivity of BLS, no additional excitation technique is required [52–54]. The BLS spectra [Fig. 2(a)] demonstrate five well-pronounced peaks in both the Stokes and anti-Stokes region. The lowest frequency peaks SS (surface Stokes) and SA (surface anti-Stokes) correspond to the modes of surface Damon-Eschbach (DE) waves propagating along the positive and negative y direction [40]. The field-swept spectra measured for different frequencies, which are vertically offset for clarity in Fig. 2(a), consist not only of DE modes but also of perpendicular standing-spin-wave (PSSW) [51,55] modes. The dashed lines correspond to the peak positions. Two peaks associated with the in-phase (acoustic) and to the out-of-phase (optic) precession of the dynamic magnetizations in two ferromagnetic films can be revealed using BLS [56–59]. Here we observed splitting of PSSW peaks for each mode to two well-defined peaks. Thus, we refer to these peaks as PS$_{nl}$ and PA$_{nl}$ for Stokes and anti-Stokes PSSW modes of nth order in the YIG layer with magnetization M_l, respectively. The frequencies of PSSW f_{ln} in the case of free surface spins [60,61] at the film surfaces were determined using the magnetic layer thickness d_l, saturation magnetization M_l, the isotropic exchange interaction, and external magnetic field H_0 [62]:

$$\omega_{ln} = \sqrt{\omega_{lnk}(\omega_{lnk} + \omega_{Ml})}, \tag{2}$$

where $\omega_{ln} = 2\pi f_{ln}$ is the angular frequency, $\omega_{lnk} = \omega_H + q\omega_{Ml}[k^2 + (n\pi/d_l)^2]$, $\omega_H = \gamma H_0$, $\omega_{Ml} = \gamma 4\pi M_l$, $q = 3 \times 10^{-12}$ cm^2 is the exchange constant [62,63], and k is the spin-wave wave number.

Figure 2(b) shows field dependencies for measured PSSW peaks PS$_{nl}$ (closed symbols) and theoretical curves plotted using Eq. (2) for $k = 0$, film thicknesses $d_1 = 54$ nm, and $d_2 = 60$ nm. At the same time, the DE dispersion curves in approximation $k \to 0$ [40] for the layers with saturation magnetization M_1 and M_2 are plotted and denoted as SS$_1$ and SS$_2$, respectively. It should be noted that DE modes are also split due to dipolar coupling, as it is shown with theoretical curves in the inset in Fig. 2(b). However, we emphasize here that the frequency resolution of 80 MHz was not sufficient to

resolve two peaks inside measured data for SS and SA peaks in Fig. 2(a).

The situation is changed when the sample was exposed with the infrared (IR) laser. An IR beam with a power of 5 mW was focused on the YIG surface into a circle of 1 mm diameter, where the BLS light beam with wavelength 532 nm was also focused [see Fig. 1(a)]. Figure 3 shows the BLS data with 45 MHz resolution without (blue curves) and with (red curves) the IR laser illumination.

Here we should note that the thermal heating of the sample could lead to the anisotropic piezoelectric effect in GaAs [64], inducing strain in YIG. This strain will induce the changes in the local magnetic field and frequencies of PSSW modes via YIG magnetoelasticity. It is also known that the magnetization of YIG is reduced with the increase of temperature, as for other magnetically ordered materials [65]. Both these effects should result in the decrease of PSSW mode frequencies ω_{ln} caused by decreasing M_l. However, the results presented in Fig. 3(a) demonstrate that the frequencies of PSSW modes are not affected by the IR laser radiation. This eliminates the effect of the significant influence of laser heating on the observed spin-wave spectra.

At the same time, the peak of the SS mode is transformed significantly. The obtained results clearly reveal two peaks inside the DE mode. The frequencies of these peaks depend on both the spin-wave wave-number value k and IR laser radiation intensity. Wave-number selectivity is achieved by the change of the incidence angle for probing laser light [51] and using the single 200-μm-diameter pinhole for wave-vector selectivity [66–69] at $k < 4$ μm^{-1}. As it is seen from Fig. 3(a), the increase of wave number from $k = 3$ μm^{-1} to $k = 11$ μm^{-1} affects only the frequencies of SS and SA peaks. SS$_1$ and SS$_2$ peaks are more distinguishable at $k = 11$ μm^{-1}. At the same time, the IR laser illumination leads to the more pronounced frequency shift of SS and SA peaks at $k = 3$ μm^{-1}. Figure 3(b) shows the BLS spectra at $k = 1.5$ μm^{-1}. It is clearly seen that the IR laser radiation leads to the significant frequency shift of Stokes peaks SS$_{1,2}$ in the case of positive orientation of the magnetic field ($H_0 = 2$ kOe) and anti-Stokes peaks SA$_{1,2}$ when the magnetic field direction is changed to the opposite ($H_0 = -2$ kOe).
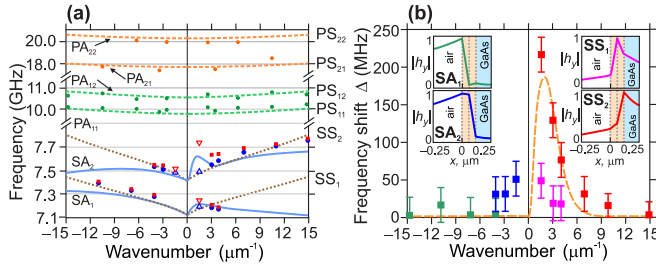
FIG. 4. (a) Spin-wave dispersion curves for YIG/GaAs with and without IR laser illumination in the external field of 2 kOe. The dashed lines indicate the result of calculation for PSSW modes. The solid curves were calculated using Eq. (3), and the dotted curves were obtained using Eq. (2). (b) The frequency shift Δ as a function of wave number. Inset: Profiles of the coupled modes of multilayer YIG/GaAs structure.

Further, we used both the diaphragm and incidence angle variation to plot the spin-wave dispersion. The BLS data in Fig. 4(a) show that PSSW mode dispersion curves (green and orange circles) are in the good accordance with the theoretical curves plotted using Eq. (2). The dotted curves in frequency range $7.1 < f < 7.8$ GHz in Fig. 4(a) are plotted using Eq. (45) from Ref. [62] for the dispersion of dipole-exchange spin waves in separate magnetic layers with magnetization M_1 and M_2. The BLS data plotted in Fig. 4 were obtained both with pinhole at $|k| \leqslant 4$ μm and variation of the in-

cidence angle $|k| > 4$ μm, with the IR laser radiation [red squares in Fig. 4(a)] and without the IR laser [blue circles in Fig. 4(a)]. It is clearly seen that the IR laser radiation leads to the significant shift of frequencies of the SS_2 mode in the dipole spin-wave region $|k| \leqslant 4$ μm. It should be also noted that the data corresponding to the peak positions for $|k| = 1.5$ μm are plotted with open triangles in both Figs. 3(b) and 4(a).

The possibility of electron-holes pair generation in GaAs under the influence of used IR radiation with $\lambda = 830$ nm results from the observed intensive absorption of radiation having $\lambda < 1$ μm in GaAs [48,70,71]. In turn, it is known that the presence of a conductive plane near a thin magnetic film perturbs the propagation of MSSW [72]. In addition, the exchange interactions can be neglected and do not influence the nonreciprocal properties of spin waves [37]. Thus, we derived Eq. (3) describing the spin-wave dispersion for a magnetostatic wave propagating in positive ($s = 1$) or negative ($s = -1$) y direction in the two-layer structure [43,73] on top of the metal screen with conductivity $\sigma(I)$, which can be varied using laser radiation with intensity I. Here $\mu_{1,2} = 1 + \omega_H \omega_{M1,2}/(\omega_H^2 - \omega^2)$, $\mu_{a1,2} = \omega \omega_{M1,2}/(\omega_H^2 - \omega^2)$, $k_s^2 = k^2 + 2j/\delta^2$, $\delta = \sqrt{c^2/(2\pi\sigma\omega)}$ is the skin depth, where c is the speed of light in vacuum. Four solid blue curves in Fig. 4(a) are plotted using Eq. (3) with fitting parameter $\sigma = 10^7$ $(\Omega \, \text{m})^{-1}$. It is seen that the spin-wave frequency shift corresponds to the case when the conductivity of the semiconductor substrate increases due to laser radiation.

$$e^{2kd_2} = \frac{[(s\mu_{a1} - \mu_1)(s\mu_{a2} - s\mu_{a1} - \mu_1 + \mu_2)e^{2kd_1} - (s\mu_{a1} + \mu_1 - 1)(s\mu_{a2} - s\mu_{a1} + \mu_1 + \mu_2)](k_s s\mu_{a2} + s^2 k - \mu_2 k_s)}{[(s\mu_{a1} - \mu_1)(s\mu_{a2} - s\mu_{a1} - \mu_1 - \mu_2)e^{2kd_1} - (s\mu_{a1} + \mu_1 - 1)(s\mu_{a2} - s\mu_{a1} + \mu_1 - \mu_2)](k_s s\mu_{a2} + s^2 k + \mu_2 k_s)} \quad (3)$$

Figure 4(b) demonstrates the frequency shift $\Delta = f_L - f_i$ as a function of the wave number, where f_L is the frequency of the peak with IR laser illumination and f_i corresponds to the peak frequency in the absence of IR radiation. The profiles of the coupled modes of a multilayer YIG/YIG/GaAs structure are shown in the inset in Fig. 4(b). The vertical dashed lines denote (from left to right) the interfaces between air, the YIG films, and between the YIG and GaAs substrate. Each experimental point in Fig. 4(b) corresponds to a frequency change of each of the above-mentioned coupled modes, as it is shown with the symbols and colors. It is seen that the propagation of $SA_{1,2}$ modes with amplitude localized at the surface with air is weakly affected by the presence of the GaAs on the opposite side. The dashed curve shows the theoretical value of $\Delta(k)$ obtained using Eq. (3). It should be noted that the proposed model for frequency shift in YIG/GaAs structure is conceivable, since it predicts the region of laser-induced frequency shift in the wave-number range of $0 < k < 4$ μm^{-1} and describes the nonreciprocal spin-wave frequency shift at negative and positive wave numbers. However, as it is shown in Fig. 4(b), the theoretically predicted frequency shift Δ is less than the experimental data at $k < 5$ μm^{-1}. This discrepancy results from the simplicity of our model that does not take into consideration some peculiarities of

the real structure and processes that could take place in it. For example, during annealing of the structure, Al atoms could diffuse from the barrier AlO_x layer to the substrate, forming $Al_xGa_{1-x}As$ alloys in the interface and thus creating conditions there for two-dimensional electron-gas (2DEG) appearance [74]. So the parameter σ should be considered just like a fitting parameter that expresses the reaction of the interface and substrate upon IR radiation in terms of single-layer conductivity. In point of fact, the conductivity value used for fitting of experimental data could not be achieved in real weakly doped GaAs, because ionization even of all atoms in the GaAs volume would not be enough for generation of the required electron-hole pair amount [75]. We also note that the BLS measurements of YIG films deposited on GGG substrates by the same technological method have not exhibited the laser-induced spin-wave nonreciprocity observed in our YIG/GaAs structure. It would thus be interesting to explore the spin-wave frequency modulation in YIG/GaAs structures with time-resolved techniques. Our results open new venues for research in that direction, and we believe that our findings open a new perspective towards the integration of magnonics in semiconductor-based devices.

In conclusion, we demonstrated by means of Brillouin light-scattering spectroscopy that the spin-wave dispersion in

thin yttrium iron garnet films on gallium arsenide substrates can be modified in a controlled manner by laser radiation. In particular, the laser-induced variation of conductivity of gallium arsenide leads to a spin-wave frequency shift in YIG of up to 225 MHz. With the proposed simple analytical theory one should be able to describe the laser-induced nonreciprocity effect. It may be a way to integrate magnonic devices in semiconductor-based electronics.

[1] ITRS, International Technology Roadmap for Semiconductors (ITRS), 2015 ed., http://www.itrs2.net/itrs-reports.html (accessed 1 April 2017) .

[2] V. V. Kruglyak, S. O. Demokritov, and D. Grundler, J. Phys. D: Appl. Phys. **43**, 264001 (2010).

[3] M. Krawczyk and D. Grundler, J. Phys.: Condens. Matter **26**, 123202 (2014).

[4] V. E. Demidov, S. Urazhdin, A. Zholud, A. V. Sadovnikov, A. N. Slavin, and S. O. Demokritov, Sci. Rep. **5**, 8578 (2015).

[5] S. A. Nikitov, D. V. Kalyabin, I. V. Lisenkov, A. N. Slavin, Y. N. Barabanenkov, S. A. Osokin, A. V. Sadovnikov, E. N. Beginin, M. A. Morozova, Y. P. Sharaevsky, Y. A. Filimonov, Y. V. Khivintsev, S. L. Vysotsky, V. K. Sakharov, and E. S. Pavlov, Phys. Usp. **58**, 1002 (2015).

[6] A. V. Chumak, V. I. Vasyuchka, A. A. Serga, and B. Hillebrands, Nat. Phys. **11**, 453 (2015).

[7] H. Yu, O. d' Allivy Kelly, V. Cros, R. Bernard, P. Bortolotti, A. Anane, F. Brandl, F. Heimbach, and D. Grundler, Nat. Commun. **7**, 11255 (2016).

[8] S. O. Demokritov, Magnons, in *Topology in Magnetism*, edited by J. Zang, V. Cros, and A. Hoffman, Springer Series in Solid-State Sciences Vol. 192 (Springer, Cham, 2018).

[9] D. Sander, S. O. Valenzuela, D. Makarov, C. H. Marrows, E. E. Fullerton, P. Fischer, J. McCord, P. Vavassori, S. Mangin, P. Pirro, B. Hillebrands, A. D. Kent, T. Jungwirth, O. Gutfleisch, C. G. Kim, and A. Berger, J. Phys. D **50**, 363001 (2017).

[10] S. O. Demokritov, *Spin Wave Confinement: Propagating Waves*, 2nd ed. (Pan Stanford Publishing, Singapore, 2017).

[11] C. S. Davies, A. Francis, A. V. Sadovnikov, S. V. Chertopalov, M. T. Bryan, S. V. Grishin, D. A. Allwood, Y. P. Sharaevskii, S. A. Nikitov, and V. V. Kruglyak, Phys. Rev. B **92**, 020408 (2015).

[12] A. V. Sadovnikov, E. N. Beginin, S. A. Odincov, S. E. Sheshukova, Y. P. Sharaevskii, A. I. Stognij, and S. A. Nikitov, Appl. Phys. Lett. **108**, 172411 (2016).

[13] S. Klingler, P. Pirro, T. Bracher, B. Leven, B. Hillebrands, and A. V. Chumak, Appl. Phys. Lett. **105**, 152410 (2014).

[14] A. Khitun, M. Bao, and K. L. Wang, J. Phys. D: Appl. Phys. **43**, 264005 (2010).

[15] A. V. Sadovnikov, S. A. Odintsov, E. N. Beginin, S. E. Sheshukova, Y. P. Sharaevskii, and S. A. Nikitov, Phys. Rev. B **96**, 144428 (2017).

[16] A. V. Sadovnikov, A. A. Grachev, S. E. Sheshukova, Y. P. Sharaevskii, A. A. Serdobintsev, D. M. Mitin, and S. A. Nikitov, Phys. Rev. Lett. **120**, 257203 (2018).

[17] Y. Kajiwara, K. Harii, S. Takahashi, J. Ohe, K. Uchida, M. Mizuguchi, H. Umezawa, H. Kawai, K. Ando, K. Takanashi, S. Maekawa, and E. Saitoh, Nature (London) **464**, 262 (2010).

[18] H. Kurebayashi, O. Dzyapko, V. E. Demidov, D. Fang, A. J. Ferguson, and S. O. Demokritov, Nat. Mater. **10**, 660 (2011).

[19] H. Nakayama, M. Althammer, Y.-T. Chen, K. Uchida, Y. Kajiwara, D. Kikuchi, T. Ohtani, S. Geprags, M. Opel, S. Takahashi, R. Gross, G. E. W. Bauer, S. T. B. Goennenwein, and E. Saitoh, Phys. Rev. Lett. **110**, 206601 (2013).

[20] M. Collet, X. de Milly, O. d'Allivy Kelly, V. V. Naletov, R. Bernard, P. Bortolotti, J. Ben Youssef, V. E. Demidov, S. O. Demokritov, J. L. Prieto, M. Muñoz, V. Cros, A. Anane, G. de Loubens, and O. Klein, Nat. Commun. **7**, 10377 (2016).

[21] V. E. Demidov, M. Evelt, V. Bessonov, S. O. Demokritov, J. L. Prieto, M. Muñoz, J. Ben Youssef, V. V. Naletov, G. de Loubens, O. Klein, M. Collet, P. Bortolotti, V. Cros, and A. Anane, Sci. Rep. **6**, 32781 (2016).

[22] T. Boudiar, B. Payet-Gervy, M.-F. Blanc-Mignon, J.-J. Rousseau, M. L. Berre, and H. Joisten, J. Magn. Magn. Mater. **284**, 77 (2004).

[23] Q. Yang, Z. Huaiwu, L. Yingli, and W. Qiye, IEEE Trans. Magn. **43**, 3652 (2007).

[24] A. K. Bandyopadhyay, S. E. Rios, S. Fritz, J. Garcia, J. Contreras, and C. J. Gutierrez, IEEE Trans. Magn. **40**, 2805 (2004).

[25] A. I. Stognij, L. V. Lutsev, V. E. Bursian, and N. N. Novitskii, J. Appl. Phys. **118**, 023905 (2015).

[26] H. Buhay, J. D. Adam, M. R. Daniel, N. J. Doyle, M. C. Driver, G. W. Eldridge, M. H. Hanes, R. L. Messham, and M. M. Sopira, IEEE Trans. Magn. **31**, 3832 (1995).

[27] X. Y. Sun, Q. Du, T. Goto, M. C. Onbasli, D. H. Kim, N. M. Aimon, J. Hu, and C. A. Ross, ACS Photonics **2**, 856 (2015).

[28] Z. Chen and V. G. Harris, J. Appl. Phys. **112**, 081101 (2012).

[29] A. Stognij, L. Lutsev, N. Novitskii, A. Bespalov, O. Golikova, V. Ketsko, R. Gieniusz, and A. Maziewski, J. Phys. D **48**, 485002 (2015).

[30] M. Munsch, N. S. Malik, E. Dupuy, A. Delga, J. Bleuse, J.-M. Gérard, J. Claudon, N. Gregersen, and J. Mørk, Phys. Rev. Lett. **110**, 177402 (2013).

[31] X. Ding, Y. He, Z.-C. Duan, N. Gregersen, M.-C. Chen, S. Unsleber, S. Maier, C. Schneider, M. Kamp, S. Höfling, C.-Y. Lu, and J.-W. Pan, Phys. Rev. Lett. **116**, 020401 (2016).

[32] T. Wolfram, J. Appl. Phys. **41**, 4748 (1970).

[33] H. van de Vaart, Electron. Lett. **6**, 601 (1970).

[34] S. R. Seshadri, Proc. IEEE **58**, 506 (1970).

[35] M. S. Sodha and N. C. Srivastava, *Microwave Propagation in Ferrimagnetics* (Springer, New York, 1981).

[36] A. G. Gurevich and G. A. Melkov, *Magnetization Oscillations and Waves* (CRC Press, New York, 1996).

[37] M. Mruczkiewicz and M. Krawczyk, Br. J. Appl. Phys. **115**, 113909 (2014).

[38] M. Mruczkiewicz, E. S. Pavlov, S. L. Vysotsky, M. Krawczyk, Y. A. Filimonov, and S. A. Nikitov, Phys. Rev. B **90**, 174416 (2014).

[39] O. Gladii, M. Haidar, Y. Henry, M. Kostylev, and M. Bailleul, Phys. Rev. B **93**, 054430 (2016).

[40] R. W. Damon and J. Eschbach, J. Phys. Chem. Solids **19**, 308 (1961).

[41] G. C. Bailey and C. Vittoria, Phys. Rev. B **8**, 3247 (1973).

[42] B. Hillebrands, Phys. Rev. B **41**, 530 (1990).

[43] S. M. Rezende, C. Chesman, M. A. Lucena, A. Azevedo, F. M. de Aguiar, and S. S. P. Parkin, J. Appl. Phys. **84**, 958 (1998).

[44] G. Bennett and J. Adam, Electron Lett. **6**, 789 (1970).

[45] Y. Toshinobu, Y. Jun-ichi, A. Kenji, and I. Jun-ichi, Jpn. J. Appl. Phys. **16**, 2187 (1977).

[46] V. G. Harris, A. Geiler, Y. Chen, S. Dae Yoon, M. Wu, A. Yang, Z. Chen, P. He, P. V. Parimi, X. Zuo, C. E. Patton, M. Abe, O. Acher, and C. Vittoria, J. Magn. Magn. Mater. **321**, 2035 (2009).

[47] K. Zeissler, M. Mruczkiewicz, S. Finizio, J. Raabe, P. M. Shepley, A. V. Sadovnikov, S. A. Nikitov, K. Fallon, S. McFadzean, S. McVitie, T. A. Moore, G. Burnell, and C. H. Marrows, Sci. Rep. **7**, 15125 (2017).

[48] W. G. Spitzer and J. M. Whelan, Phys. Rev. **114**, 59 (1959).

[49] B. P. Zakharchenya and V. L. Korenev, Phys. Usp. **48**, 603 (2005).

[50] J. Jorzick, S. O. Demokritov, C. Mathieu, B. Hillebrands, B. Bartenlian, C. Chappert, F. Rousseaux, and A. N. Slavin, Phys. Rev. B **60**, 15194 (1999).

[51] S. O. Demokritov, B. Hillebrands, and A. N. Slavin, Phys. Rep. **348**, 441 (2001).

[52] J. Sandercock, Opt. Commun. **2**, 73 (1970).

[53] J. Sandercock and W. Wettling, IEEE Trans. Magn. **14**, 442 (1978).

[54] C. E. Patton, Phys. Rep. **103**, 251 (1984).

[55] C. Bayer, J. Jorzick, B. Hillebrands, S. O. Demokritov, R. Kouba, R. Bozinoski, A. N. Slavin, K. Y. Guslienko, D. V. Berkov, N. L. Gorn, and M. P. Kostylev, Phys. Rev. B **72**, 064427 (2005).

[56] P. Grünberg, J. Appl. Phys **51**, 4338 (1980).

[57] P. Grünberg, M. G. Cottam, W. Vach, C. Mayr, and R. E. Camley, J. Appl. Phys **53**, 2078 (1982).

[58] J. F. Cochran and J. R. Dutcher, J. Appl. Phys. **64**, 6092 (1988).

[59] P. A. Grünberg, Rev. Mod. Phys. **80**, 1531 (2008).

[60] G. Rado and J. Weertman, J. Phys. Chem. Solids **11**, 315 (1959).

[61] K. Y. Guslienko and A. N. Slavin, Phys. Rev. B **72**, 014463 (2005).

[62] B. A. Kalinikos and A. N. Slavin, J. Phys. C: Solid State Phys. **19**, 7013 (1986).

[63] D. T. Edmonds and R. G. Petersen, Phys. Rev. Lett. **2**, 499 (1959).

[64] S. C. Masmanidis, R. B. Karabalin, I. D. Vlaminck, G. Borghs, M. R. Freeman, and M. L. Roukes, Science **317**, 780 (2007).

[65] S. Chikazumi, *Physics of Ferromagnetism,* 2nd ed. (Oxford University Press, Oxford, UK, 1997).

[66] V. N. Venitsky, V. V. Eremenko, and E. V. Matyushkin, JETP Lett. **27**, 222 (1978).

[67] W. Wettling, W. D. Wilber, P. Kabos, and C. E. Patton, Phys. Rev. Lett. **51**, 1680 (1983).

[68] G. Srinivasan, C. E. Patton, and P. R. Emtage, J. Appl. Phys. **61**, 2318 (1987).

[69] H. Xia, P. Kabos, H. Y. Zhang, P. A. Kolodin, and C. E. Patton, Phys. Rev. Lett. **81**, 449 (1998).

[70] M. Masuda, N. S. Chang, and Y. Matsuo, IEEE Trans. Microw. Theory Techn. **22**, 132 (1974).

[71] A. Kindyak, Mater. Lett. **24**, 359 (1995).

[72] R. E. D. Wames and T. Wolfram, Br. J. Appl. Phys. **41**, 5243 (1970).

[73] W. L. Bongianni, J. Appl. Phys. **43**, 2541 (1972).

[74] A. A. Shevyrin, A. G. Pogosov, A. K. Bakarov, and A. A. Shklyaev, Phys. Rev. Lett **117**, 017702 (2016).

[75] M. Levinshtein, S. Rumyantsev, and M. Shur, *Handbook Series on Semiconductor Parameters* (World Scientific, London, 1996), Vol. 1.